Structural Engineering and Mechanics, *Vol. 67, No. 3 (2018) 219-232*
DOI: https://doi.org/10.12989/sem.2018.67.3.219

A novel shear and normal deformation theory for hygrothermal bending response of FGM sandwich plates on Pasternak elastic foundation

Mohammad Alakel Abazid[∗1], Muneerah S. Alotebi[2a] and Mohammed Sobhy[1,3b]

[1]*Department of Mathematics and Statistics, Faculty of Science, King Faisal University, P.O. Box 400, Hofuf, 31982, Saudi Arabia*
[2]*Department of Mathematics, Faculty of Arts and Science at Nairiyah, Hafr Al Batin University, P.O. Box 1803, Hafr Al Batin 31991, Saudi Arabia*
[3]*Department of Mathematics, Faculty of Science, Kafrelsheikh University, Kafrelsheikh 33516, Egypt*

(Received March 25, 2018, Revised May 9, 2018, Accepted May 13, 2018)

Abstract. This paper deals with the static bending of various types of FGM sandwich plates resting on two-parameter elastic foundations in hygrothermal environment. The elastic foundation is modeled as Pasternak's type, which can be either isotropic or orthotropic and as a special case, it converges to Winkler's foundation if the shear layer is neglected. The present FGM sandwich plate is assumed to be made of a fully ceramic core layer sandwiched by metal/ceramic FGM coats. The governing equations are derived from principle of virtual displacements based on a shear and normal deformations plate theory. The present theory takes into account both shear and normal strains effects, thus it predicts results more accurate than the shear deformation plate theories. The results obtained by the shear and normal deformation theory are compared with those available in the literature and also with those obtained by other shear deformation theories. It is concluded that the present results are slightly deviated from other results because the normal deformation effect is taken into account. Numerical results are presented to show the effects of the different parameters, such as side-to-thickness ratio, foundation parameters, aspect ratio, temperature, moisture, power law index and core thickness on the stresses and displacements of the FG sandwich plates.

Keywords: sandwich plates; shear and normal deformation theory; hygrothermal bending; Pasternak foundation

1. Introduction

Sandwich structures are composed of three different homogeneous layers bonded together in order to get more enhanced mechanical and thermal properties, namely, a core layer covered by two face sheets. However, a sudden change in material properties occurs at the interfaces of the sandwich plate. To overcome this problem, Zenkour (2005) introduced an FGM sandwich plates. He assumed that the core layer is composed of a fully homogeneous ceramic while the face layers are made of FGMs in which the material properties vary through the thickness only with regard to a power law distribution as a function of the volume fractions of the constituents. In this study, the top and bottom surfaces of the sandwich plate are assumed to be full metal material. The material properties of the face sheets are smoothly graded in the thickness direction from the top and bottom surfaces (fully metal) to the interfaces, which are fully ceramic material. Another type of FGM sandwich plates are developed by using an FGM core and homogeneous face sheets (Anderson 2003, Kirugulige *et al.* 2005, Fard 2014).

Anderson (2003) introduced an analytical 3-D solution for an FGM sandwich plate which is subjected to transverse loading by a rigid sphere and obtained the stresses and displacements with varying the core stiffness. In this investigation, the sandwich plate is composed of orthotropic face layers with an isotropic FGM core, in which the properties vary exponentially in the z-axis direction. The main equations are deduced by employing Reissner functional. Thermo-elastic analysis of a sandwich plate made of orthotropic stiff face sheets bonded to a soft FGM core has been presented by Das *et al.* (2006). Kashtalyan and Menshykova (2009) introduced 3-D elasticity analysis for static bending of sandwich plates with FGM core subjected to transverse loading. Free vibration of sandwich cylindrical plates with FG core based on power-law distribution has been investigated by Aragh *et al.* (2011) using the differential quadrature method to solve the governing differential equations. Dozio (2013) presented an advanced 2-D Ritz-based models to study the natural frequencies of sandwich panels with FGM core. Alibeigloo and Liew (2014) developed an exact 3-D solution for free vibration of sandwich cylindrical panels with FGM core. Zenkour and Alghamdi (2008) studied the thermoelastic bending analysis FG sandwich plates. Zenkour (2007) studied the bending response of the rotating FG annular disk with rigid casing. Cheng and Batra (2000) investigated the buckling and natural frequency of an FG plate by employing the third-order plate theory.

In addition, several studies have been devoted to investigate the behavior of the sandwich plates with FGM face sheets (Tounsi *et al.* 2016, Bouderba *et al.* 2016, Cunedioglu 2015). Zenkour (2005) illustrated the static

∗Corresponding author, Ph.D.
E-mail: mabazid@kfu.edu.sa or mhdabazid@gmail.com
[a]M.Sc. Student
[b]Associate Professor

ISSN: 1225-4568 (Print), 1598-6217 (Online)

bending, mechanical buckling and natural frequency of several types of FGM sandwich plates. He derived the equations of motions based on Hamilton's principle and obtained the analytical solution using Navier's method. Based on Ritz method and Chebhyshev polynomial series, Li *et al.* (2008) solved the three-dimensional motion equations to obtain the frequencies of simply supported and clamped FGM sandwich plates. The stresses, deflection, and vibration of FGM sandwich plates have been illustrated by Natarajan and Manickam (2012) using higher-order zigzag theory. Based on the exponential distribution law developed by Sobhy (2013). For the material properties of the sandwich plates, the buckling and free vibration of FGM sandwich panels were investigated by Sobhy (2013), Meziane *et al.* (2014) and Sofiyev (2014). The bending analysis of FGM viscoelastic sandwich structures resting on Winkler-Pasternak elastic foundations was presented by Zenkour *et al.* (2010) and Zenkour and Sobhy (2012). Chen *et al.* (2017) investigated the thermal influence on the vibration and stability of FGM sandwich plates with FG face sheets. Meksi *et al.* (2017) proposed a new shear deformation plate theory to investigate the various behavior of FGM sandwich plates. Radwan (2017) illustrated the nonlinear hygrothermal effects on the buckling of the FGM plates resting on elastic foundations. Li *et al.* (2018) investigated the thermomechanical effects on the bending of FGM sandwich plates with both FG face sheets and FG core.

In the past few decades, a significant number of different plate theories have been developed to analyze FGMs and represent the kinematics of deformation. The classical plate theory (CPT) is the most well-known and widely used one in this context. It considers an extension of the Kirchhoff-Love assumptions for the isotropic plate. Moreover, it is convenient to analyze thin plates, where straight lines or planes normal to the neutral plate axis will remain straight and normal after deformation. However, it is not convenient for the moderately thick and thick plates, where the shear effects should be considered. In other words, this CPT neglects the effect of transverse shear deformation (1945). Consequently, the first order shear deformation theory (FSDT) has been developed to consider the transvers shear effects while shear correction factors (SCFs) should be added to compute the shear energy accurately. SCFs are based on the boundary conditions, geometries, and the material properties of the problem handled (2003).

In order to eliminate the use of the SCFs, higher-order shear deformation theories (HSDTs) were devised using various shape functions. The aforementioned three theories which are the classical plate theory (CPT), the first order shear deformation, and the higher order shear deformation theory (HSDT) were all applied on isotropic, classical and advanced composite beams, plates and shells. Zenkour (2009a) has also introduced the sinusoidal shear deformation plate theory (SPT) using trigonometric terms for the displacements. In his study, the shear stresses are distributed through the thickness of the plate as a cosine function, and they vanish at the top and bottom surface of the plate. Moreover, there is no need for a correction factor in the sinusoidal theory. The sinusoidal theory and some other higher order theories have been employed by Arefi and Zenkour (2016, 2017a, b, c, d, e, f, g, h, i, j), Zenkour and Arefi (2017) and Arefi *et al.* (2018) to illustrate the various behaviors of the FG nano/microscale plates and beams and also FG piezoelectric nanoplates. Carrera (2002) and Carrera and Ciuffreda (2005) presented a unified formulation for various higher order shear deformation plate theories. Sobhy and Radwan (2017) presented a new quasi-3D nonlocal hyperbolic plate theory to study the vibration and buckling of FGM nanoplates. Bouafia *et al.* (2017) introduced a nonlocal quasi-3D theory to illustrate the bending and free vibration of nanobeams.

Several higher-order plate theories namely Reddy (1984), Touratier (1991), Soldatos (1992), Karama *et al.* (2003) and Aydogdu (2009) have been arisen to overcome the inadequacy of the CPT and FSDT. However, the higher-order plate theories contain at least five unknown functions, thus five governing equations are obtained. Despite the effectiveness and accuracy of the higher-order plate theories, many researchers devoted their efforts to improve these theories by reducing the number of unknowns and then reducing the mathematical processing. A two-unknown shear deformation plate theory was developed by Shimpi (2003) for homogeneous plates containing only two unknown functions. For heterogeneous plates and based on the assumptions of Shimpi's theory, many authors say Tounsi *et al.* (2013) and Thai and Vo (2013) extended this theory to contain four functions. Recently, Sobhy (2016) has successfully reformulated Shimpi's theory by introducing a four-unknown shear deformation plate theory with a new shape function, which is initially applied to the buckling and vibration of FGM sandwich plates. It reveals that this theory is more reliable and highly accurate than many other shear deformation plate theories.

This work aims to introduce a new shear and normal deformations five-variable plate theory that is employed here to analyze the bending behavior of FGM sandwich plate. The present plate is assumed to be resting on two-parameter elastic foundations and subjected to transverse mechanical, thermal and moisture loads at the top surface of the plate. The FGM sandwich plate is made of a fully ceramic core layer integrated by metal/ceramic FGM layers. Utilizing the principle of virtual displacements, the governing equations of the static response of non-homogeneous composite plates are derived containing the elastic foundation interaction. In accordance with the suggested theory, five differential equations are obtained. These equations are then solved for simply supported FGM sandwich plate based on Navier type solution. Numerical results for the bending of several types of symmetric FGM sandwich plates are presented. The validity of the present solution is demonstrated by comparison with solutions available in the literature. The influences of the inhomogeneity parameter, aspect ratio, thickness ratio and the foundation parameters on the deflection and stresses are investigated.

2. Mathematical model

Assume a rectangular sandwich plate composed of three

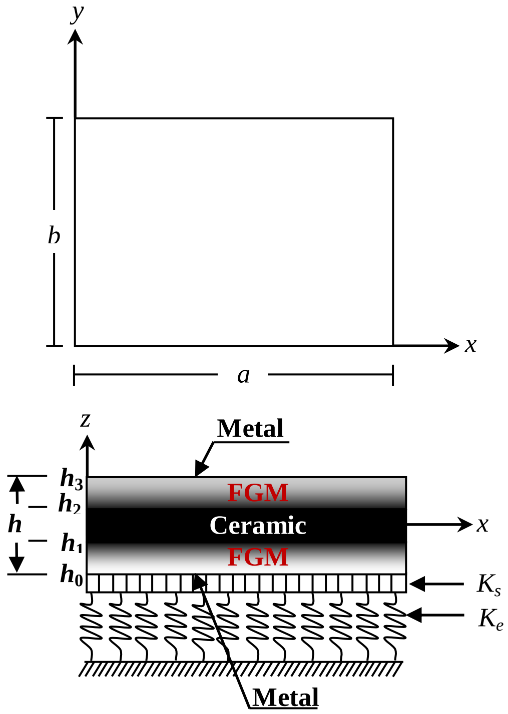

Fig. 1 Configuration and coordinate system for an FGM sandwich plate resting on Pasternak foundation

elastic layers that are made of functionally graded material of length a, width b and thickness h, reference to a rectangular coordinates (x,y,z) as shown in Fig. 1. Material properties at a point in the plate are commonly assumed to be given by the rule of mixture (Zenkour 2005, 2009a, b and Houari *et al.* 2013).

$$P^{(n)}(z) = P_m + (P_c - P_m)V^{(n)}, \qquad n = 1,2,3, \tag{1}$$

where P represents the material properties such as Young's modulus E, thermal expansion coefficient α, moisture expansion coefficient η and mass density ρ, while Poisson's ratio ν is taken a constant value. The subscripts m and c stand for metal and ceramic materials. The volume fraction of the layer n is $V^{(n)}$ that is given as a simple power law through the thickness. It reads (Zenkour 2005, 2009b)

$$\begin{aligned} V^{(1)} &= \left(\frac{z-h_0}{h_1-h_0}\right)^k, && h_0 \le z \le h_1, \\ V^{(2)} &= 1, && h_1 \le z \le h_2, \\ V^{(3)} &= \left(\frac{z-h_3}{h_2-h_3}\right)^k, && h_2 \le z \le h_3, \end{aligned} \tag{2}$$

where k is the power law index, $0 \le k < \infty$. Note that, when $k = 0$, the plate is composed of a homogeneous ceramic material. While, when k trendsinfinity, one obtain a metal-ceramic-metal sandwich plate. The sandwich plate is assumed to be resting on two layers of foundations. The first layer consists of a set of springs that are connected in parallel (see, Fig. 1). While, the second represents a shear layer. The interaction between the sandwich plate and Pasternak foundation can be given as (Abazid and Sobhy 2018 and Sobhy 2017)

$$R = [K_e u_3 - K_s \nabla^2 u_3]_{z=-\frac{h}{2}}, \tag{3}$$

where R represents the foundation reaction force per unit area; K_e is springs coefficients, while K_s is shear layer coefficients the function u_3 is the transverse displacement. The displacement components u_1, u_2 and u_3 in the x, y and z directions, respectively, at any point in the plate, can be written as

$$\begin{aligned} u_1 &= u_0(x,y) - z\frac{\partial w_b}{\partial x} - \Phi(z)\frac{\partial w_s}{\partial x}, \\ u_2 &= v_0(x,y) - z\frac{\partial w_b}{\partial y} - \Phi(z)\frac{\partial w_s}{\partial y}, \\ u_3 &= w_b(x,y) + w_s(x,y) + w_{st}(x,y,z), \end{aligned} \tag{4}$$

where $\Phi(z) = z - \varphi(z)$, $w_{st}(x,y,z) = g(z)\psi_z(x,y)$.

The additional displacement ψ_z accounting for the effect of normal stress is included and $g(z)$ is defined as follows

$$g(z) = \varphi'(z),$$

in which the shape function $\varphi(z)$ is given for the present theory as $\varphi(z) = z/(1+4z^2/h^2)$, while for the third-order plate theory (TPT) (Reddy 1984), it is expressed as $\varphi(z) = z - 4z^3/3h^2$, and for the sinusoidal plate theory (SPT) (Touratier 1991), it is defined as $\varphi(z) = \frac{h}{\pi}\sin\left(\frac{z\pi}{h}\right)$.

The strain components which are related to the displacements given in Eq. (4), can be expressed as

$$\begin{Bmatrix} \varepsilon_x \\ \varepsilon_y \\ \varepsilon_{xy} \end{Bmatrix} = \begin{Bmatrix} \varepsilon_x^0 \\ \varepsilon_y^0 \\ \varepsilon_{xy}^0 \end{Bmatrix} + z\begin{Bmatrix} k_x^b \\ k_y^b \\ k_{xy}^b \end{Bmatrix} + \Phi(z)\begin{Bmatrix} k_x^s \\ k_y^s \\ k_{xy}^s \end{Bmatrix}, \qquad \begin{Bmatrix} \varepsilon_{yz} \\ \varepsilon_{xz} \end{Bmatrix} = g(z)\begin{Bmatrix} \varepsilon_{yz}^0 \\ \varepsilon_{xz}^0 \end{Bmatrix}, \qquad \varepsilon_z = g'(z)\varepsilon_z^0, \tag{5}$$

where

$$\begin{aligned} &\varepsilon_x^0 = \frac{\partial u_0}{\partial x}, \quad \varepsilon_y^0 = \frac{\partial v_0}{\partial y}, \quad \varepsilon_{xy}^0 = \frac{\partial u_0}{\partial y} + \frac{\partial v_0}{\partial x}, \\ &k_x^b = -\frac{\partial^2 w_b}{\partial x^2}, \quad k_y^b = -\frac{\partial^2 w_b}{\partial y^2}, \quad k_{xy}^b = -2\frac{\partial^2 w_b}{\partial x \partial y}, \\ &k_x^s = -\frac{\partial^2 w_s}{\partial x^2}, \quad k_y^s = -\frac{\partial^2 w_s}{\partial y^2}, \quad k_{xy}^s = -2\frac{\partial^2 w_s}{\partial x \partial y}, \\ &\varepsilon_{yz}^0 = \frac{\partial w_s}{\partial y} + \frac{\partial \psi_z}{\partial y}, \quad \varepsilon_{xz}^0 = \frac{\partial w_s}{\partial x} + \frac{\partial \psi_z}{\partial x}, \varepsilon_z^0 = \psi_z, \end{aligned} \tag{6}$$

$$g'(z) = \frac{\mathrm{d}g(z)}{\mathrm{d}z}.$$

The stress-strain relations for a linear elastic sandwich plate are expressed as

$$\begin{Bmatrix} \sigma_x \\ \sigma_y \\ \sigma_z \\ \sigma_{yz} \\ \sigma_{xz} \\ \sigma_{xy} \end{Bmatrix}^{(n)} = \begin{bmatrix} c_{11} & c_{12} & c_{13} & 0 & 0 & 0 \\ c_{12} & c_{22} & c_{23} & 0 & 0 & 0 \\ c_{13} & c_{23} & c_{33} & 0 & 0 & 0 \\ 0 & 0 & 0 & c_{44} & 0 & 0 \\ 0 & 0 & 0 & 0 & c_{55} & 0 \\ 0 & 0 & 0 & 0 & 0 & c_{66} \end{bmatrix}^{(n)} \tag{7}$$

$$\times\begin{Bmatrix} \varepsilon_x-\alpha^{(n)}\Delta T-\eta^{(n)}\Delta H \\ \varepsilon_y-\alpha^{(n)}\Delta T-\eta^{(n)}\Delta H \\ \varepsilon_z-\alpha^{(n)}\Delta T-\eta^{(n)}\Delta H \\ \varepsilon_{yz} \\ \varepsilon_{xz} \\ \varepsilon_{xy} \end{Bmatrix},$$

where

$$c_{11}=c_{22}=c_{33}=\frac{(1-v)E(z)}{(1+v)(1-2v)},\quad c_{12}=c_{13}=c_{23}=\frac{vE(z)}{(1+v)(1-2v)},\quad c_{44}=c_{55}=c_{66}=\frac{E(z)}{2(1+v)}. \tag{8}$$

3. Governing equations

The principle of virtual displacements in this case can be expressed as (Arefi and Zenkour 2018)

$$c_{11}=c_{22}=c_{33}=\frac{(1-v)E(z)}{(1+v)(1-2v)},\quad c_{12}=c_{13}=c_{23}=\frac{vE(z)}{(1+v)(1-2v)},\quad c_{44}=c_{55}=c_{66}=\frac{E(z)}{2(1+v)}. \tag{9}$$

where Ω is the top surface, h_n and h_{n-1} $(n=1,2,3)$ are the top and bottom z-coordinates of the nth layer. By substituting Eq. (5) into Eq. (9), the principle of virtual displacements can be rewritten as

$$\int_\Omega \left(N_x\delta\varepsilon_x^0+N_y\delta\varepsilon_y^0+N_z\delta\varepsilon_z^0+N_{xy}\delta\varepsilon_{xy}^0+M_x^b\delta k_x^b+M_y^b\delta k_y^b+M_{xy}^b\delta k_{xy}^b+M_x^s\delta k_x^s+M_y^s\delta k_y^s+M_{xy}^s\delta k_{xy}^s+R_{xz}^s\delta\varepsilon_{xz}^0+R_{yz}^s\delta\varepsilon_{yz}^0\right)\mathrm{d}\Omega\mathrm{d}z+\int_\Omega (R-q)\,\delta u_3|_{z=-h/2}\mathrm{d}\Omega=0, \tag{10}$$

where

$$\begin{Bmatrix} N_{xx}, & N_{yy}, & N_{xy} \\ M_{xx}^b, & M_{yy}^b, & M_{xy}^b \\ M_{xx}^s, & M_{yy}^s, & M_{xy}^s \end{Bmatrix}=\sum_{n=1}^{3}\int_{h_{n-1}}^{h_n}\left(\sigma_x,\sigma_y,\sigma_{xy}\right)^{(n)}\begin{Bmatrix} 1 \\ z \\ \Phi(z)\end{Bmatrix}dz, \tag{11}$$

$$\left(R_{xz}^s,R_{yz}^s\right)=\sum_{n=1}^{3}\int_{h_{n-1}}^{h_n}\left(\sigma_{xz},\sigma_{yz}\right)^{(n)}g(z)dz,$$

$$N_z=\sum_{n=1}^{3}\int_{h_{n-1}}^{h_n}\sigma_z{}^{(n)}g'(z)dz.$$

Integrating Eq. (10) by parts and setting the coefficients $\delta u_0,\delta v_0,\delta w_b,\delta w_s$ and $\delta\psi_z$ equal to zero, separately, yields the governing equations as

$$\frac{\partial N_{xx}}{\partial x}+\frac{\partial N_{xy}}{\partial y}=0,$$
$$\frac{\partial N_{xy}}{\partial x}+\frac{\partial N_{yy}}{\partial y}=0,$$
$$\frac{\partial^2 M_{xx}^b}{\partial x^2}+2\frac{\partial^2 M_{xy}^b}{\partial x\partial y}+\frac{\partial^2 M_{yy}^b}{\partial y^2}+q-R=0, \tag{12}$$
$$\frac{\partial^2 M_{xx}^s}{\partial x^2}+2\frac{\partial^2 M_{xy}^s}{\partial x\partial y}+\frac{\partial^2 M_{yy}^s}{\partial y^2}+\frac{\partial R_{xz}^s}{\partial x}+\frac{\partial R_{yz}^s}{\partial y}+q-R=0,$$
$$\frac{\partial R_{xz}^s}{\partial x}+\frac{\partial R_{yz}^s}{\partial y}-N_z=0.$$

By incorporating Eq. (7) into Eq. (11), the stress resultants of the FGM sandwich plate can be related to the total strains as

$$\begin{Bmatrix} N \\ M^b \\ M^s \end{Bmatrix}=\begin{bmatrix} A & B & B^s \\ B & D & D^s \\ B^s & D^s & H^s \end{bmatrix}\begin{Bmatrix} \varepsilon \\ k^b \\ k^s \end{Bmatrix}+\begin{Bmatrix} F \\ F^s \\ Q \end{Bmatrix}\varepsilon_z^0-\begin{Bmatrix} N^T \\ M^{bT} \\ M^{sT} \end{Bmatrix}-\begin{Bmatrix} N^H \\ M^{bH} \\ M^{sH} \end{Bmatrix}, \tag{13}$$

$$\left(R_{yz}^s,R_{xz}^s\right)=A_{44}^s\left(\varepsilon_{yz}^0,\varepsilon_{xz}^0\right),$$

$$N_z=Q^s\psi_z+F_{xx}\left(\varepsilon_x^0+\varepsilon_y^0\right)+F_{xx}^s\left(k_x^b+k_y^b\right)+Q_{xx}\left(k_x^s+k_y^s\right)-N_z^T-N_z^H,$$

where

$$N=\left\{N_{xx},N_{yy},N_{xy}\right\}^t,\ M^b=\left\{M_{xx}^b,M_{yy}^b,M_{xy}^b\right\}^t,\ M^s=\left\{M_{xx}^s,M_{yy}^s,M_{xy}^s\right\}^t, \tag{14a}$$

$$N^T=\left\{N_{xx}^T,N_{yy}^T,0\right\}^t,\ M^{bT}=\left\{M_{xx}^{bT},M_{yy}^{bT},0\right\}^t,\ M^{sT}=\left\{M_{xx}^{sT},M_{yy}^{sT},0\right\}^t, \tag{14b}$$

$$\varepsilon=\left\{\varepsilon_x^0,\varepsilon_y^0,\varepsilon_{xy}^0\right\}^t,\ k^b=\left\{k_x^b,k_y^b,k_{xy}^b\right\}^t,\ k^s=\left\{k_x^s,k_y^s,k_{xy}^s\right\}^t, \tag{14c}$$

$$F=\left\{F_{xx},F_{yy},0\right\}^t,\ F^s=\left\{F_{xx}^s,F_{yy}^s,0\right\}^t,\ Q=\left\{Q_{xx},Q_{yy},0\right\}^t, \tag{14d}$$

$$A=\begin{bmatrix} A_{11} & A_{12} & 0 \\ A_{12} & A_{22} & 0 \\ 0 & 0 & A_{66} \end{bmatrix},\ B=\begin{bmatrix} B_{11} & B_{12} & 0 \\ B_{12} & B_{22} & 0 \\ 0 & 0 & B_{66} \end{bmatrix},\ D=\begin{bmatrix} D_{11} & D_{12} & 0 \\ D_{12} & D_{22} & 0 \\ 0 & 0 & D_{66} \end{bmatrix}, \tag{14e}$$

$$B^s=\begin{bmatrix} B_{11}^s & B_{12}^s & 0 \\ B_{12}^s & B_{22}^s & 0 \\ 0 & 0 & B_{66}^s \end{bmatrix},\ D^s=\begin{bmatrix} D_{11}^s & D_{12}^s & 0 \\ D_{12}^s & D_{22}^s & 0 \\ 0 & 0 & D_{66}^s \end{bmatrix},\ H^s=\begin{bmatrix} H_{11}^s & H_{12}^s & 0 \\ H_{12}^s & H_{22}^s & 0 \\ 0 & 0 & H_{66}^s \end{bmatrix}, \tag{14f}$$

where the plate stiffness $A_{ij},B_{ij},etc.$ are given by

$$\begin{Bmatrix} A_{11}, & B_{11}, & D_{11}, B_{11}^s, & D_{11}^s, & H_{11}^s \\ A_{12}, & B_{12}, & D_{12}, B_{12}^s, & D_{12}^s, & H_{12}^s \\ A_{66}, & B_{66}, & D_{66}, B_{66}^s, & D_{66}^s, & H_{66}^s \end{Bmatrix} = \sum_{n=1}^{3} \int_{h_{n-1}}^{h_n} c_{11}^{(n)} \left(1, z, z^2, \Phi(z), z\Phi(z), \Phi^2(z)\right) \times \begin{Bmatrix} 1 \\ \nu \\ \dfrac{1-\nu}{2} \end{Bmatrix} \mathrm{d}z, \tag{15a}$$

$$(A_{22}, B_{22}, D_{22}, B_{22}^s, D_{22}^s, H_{22}^s) = (A_{11}, B_{11}, D_{11}, B_{11}^s, D_{11}^s, H_{11}^s), \tag{15b}$$

$$A_{44}^s = A_{55}^s = \sum_{n=1}^{3} \int_{h_{n-1}}^{h_n} \frac{E^{(n)}(z)}{2(1+v)} [g(z)]^2 \mathrm{d}z, \tag{15c}$$

$$\{F_{xx}, F_{xx}^s, Q_{xx}, Q^s\} = \sum_{n=1}^{3} \int_{h_{n-1}}^{h_n} \frac{vE^{(n)} g'(z)}{1-v^2} \left\{1, z, \Phi(z), \frac{g'(z)}{v}\right\} \mathrm{d}z, \tag{15d}$$

$$F_{yy} = F_{xx}, \qquad F_{yy}^s = F_{xx}^s, \qquad Q_{yy} = Q_{xx}.$$

The stress and moment resultants $N_{xx}^{\Theta} = N_{yy}^{\Theta}, M_{xx}^{b\Theta} = M_{yy}^{b\Theta}$, and $M_{xx}^{s\Theta} = M_{yy}^{s\Theta}$ and $N_z^{\Theta}, \Theta = T, H)$ due to thermal and humidity loadings are expressed by

$$\begin{Bmatrix} N_{xx}^T \\ M_{xx}^{bT} \\ M_{xx}^{sT} \\ N_z^T \end{Bmatrix} = \sum_{n=1}^{3} \int_{h_{n-1}}^{h_n} \frac{E^{(n)}(z)}{1-v^2} (1 + 2v) \alpha^{(n)}(z) \Delta T \begin{Bmatrix} 1 \\ z \\ \Phi(z) \\ g'(z) \end{Bmatrix} \mathrm{d}z, \tag{16}$$

$$\begin{Bmatrix} N_{xx}^H \\ M_{xx}^{bH} \\ M_{xx}^{sH} \\ N_z^H \end{Bmatrix} = \sum_{n=1}^{3} \int_{h_{n-1}}^{h_n} \frac{E^{(n)}(z)}{1-v^2} (1 + 2v) \eta^{(n)}(z) \Delta H \begin{Bmatrix} 1 \\ z \\ \Phi(z) \\ g'(z) \end{Bmatrix} \mathrm{d}z. \tag{17}$$

The applied temperature $T(x, y, z, t)$ and the moisture concentration $H(x, y, z, t)$ are assumed to be nonlinearly distributed through the thickness as (Zenkour 2004)

$$\Theta(x, y, z, t) = \Theta_1(x, y, t) + \frac{z}{h} \Theta_2(x, y, t) + \frac{\varphi(z)}{h} \Theta_3(x, y, t), \tag{18}$$

$$\Theta = T, H.$$

4. Exact solution for FGM sandwich plates

In this section, we obtain the exact solution for the bending of rectangular FGM sandwich plates when the four edges are all simply supported. To solve the governing partial differential Eqs. (12), the boundary conditions at the side edges, for the present four-unknown plate theory, are given as

$$v_0 = w_b = w_s = \frac{\partial w_b}{\partial y} = \frac{\partial w_s}{\partial y} = \psi_z = N_{xx} = M_{xx}^b = M_{xx}^s = 0, \text{ at } x = 0, a, \tag{19a}$$

$$u_0 = w_b = w_s = \frac{\partial w_b}{\partial x} = \frac{\partial w_s}{\partial x} = \psi_z = N_{yy} = M_{yy}^b = M_{yy}^s = 0, \text{ at } y = 0, b. \tag{19b}$$

To satisfy the above boundary conditions, Navier method assumed that the displacement components are given in the form of double trigonometric series as

$$\begin{Bmatrix} u_0 \\ v_0 \\ w_b \\ w_s \\ \psi_z \end{Bmatrix} = \begin{Bmatrix} U_{mr} \cos(\theta x) \sin(\vartheta y) \\ V_{mr} \sin(\theta x) \cos(\vartheta y) \\ W_{mrb} \sin(\theta x) \sin(\vartheta y) \\ W_{mrs} \sin(\theta x) \sin(\vartheta y) \\ Z_{mr} \sin(\theta x) \sin(\vartheta y) \end{Bmatrix}, \tag{20}$$

where $U_{mr}, V_{mr}, W_{mrb} W_{mrs}$, and Z_{mr} are arbitrary parameters; $\theta = \frac{m\pi}{a}$ and $\vartheta = \frac{r\pi}{b}$. Further, according to Navier solution, the transverse mechanical and hygrothermal loads are given in the following form

$$\begin{Bmatrix} q \\ T_1 \\ T_2 \\ T_3 \\ H_1 \\ H_2 \\ H_3 \end{Bmatrix} = \begin{Bmatrix} q_0 \\ t_1 \\ t_2 \\ t_3 \\ c_1 \\ c_2 \\ c_3 \end{Bmatrix} \sin(\theta x) \sin(\vartheta y), \tag{21}$$

where $q_0, t_1, t_2, t_3, c_1, c_2$ and c_3 are constants.

Incorporating Eqs. (20) and (21) into Eq. (12) with the help of Eqs. (13) and (14) yields the following operator equation,

$$[P]\{\Delta\} = \{L\}, \tag{22}$$

where $\{\Delta\} = \{U_{mr}, V_{mr}, W_{mrb}, W_{mrs}, Z_{mr}\}^t$ and the elements P_{ij} and L_i are expressed as

$$\begin{aligned} P_{11} &= \theta^2 A_{11} + \vartheta^2 A_{66}, \\ P_{12} &= \theta\vartheta(A_{12} + A_{66}), \\ P_{13} &= -\theta(\theta^2 B_{11} + \vartheta^2 B_{12} + 2\vartheta^2 B_{66}), \\ P_{14} &= -\theta(\theta^2 B_{11}^s + \vartheta^2 B_{12}^s + 2\vartheta^2 B_{66}^s, \\ P_{15} &= -F_1\theta, \\ P_{22} &= \theta^2 A_{66} + \vartheta^2 A_{11}, \\ P_{23} &= -\vartheta(\theta^2 B_{12} + 2\theta^2 B_{66} + \vartheta^2 B_{11}), \\ P_{24} &= -\vartheta(\theta^2 B_{12}^s + 2\theta^2 B_{66}^s + \vartheta^2 B_{11}^s), \end{aligned} \tag{23}$$

$$P_{25} = -F_1\vartheta,$$

$$P_{33} = K_1 - (-\theta^2 - \vartheta^2)K_2 + D_{11}\theta^4 + 2D_{12}\theta^2\vartheta^2 + 4D_{66}\theta^2\vartheta^2 + D_{11}\vartheta^4,$$

$$P_{34} = K_1 - (-\theta^2 - \vartheta^2)K_2 + D_{11}^s\theta^4 + 2D_{12}^s\theta^2\vartheta^2 + 4D_{66}^s\theta^2\vartheta^2 + D_{11}^s\vartheta^4,$$

$$P_{35} = F_s(\theta^2 + \vartheta^2),$$

$$P_{44} = K_1 - (\theta^2 - \vartheta^2)K_2 + H_{11}^s\theta^4 + H_{12}^s\theta^2\vartheta^2 + 4H_{66}^s\theta^2\vartheta^2 + H_{11}^s\vartheta^4 + \theta^2 A_{44}^s + \vartheta^2 A_{44}^s,$$

$$P_{45} = (\theta^2 + \vartheta^2)(Q_1 + A_{44}^s),$$

$$P_{55} = \theta^2 A_{44}^s + \vartheta^2 A_{44}^s + Q_s,$$

$$L_1 = -\theta(A_1t_1 + A_2t_2 + A_3t_3 + H_1c_1 + H_2c_2 + H_3c_3,$$

$$L_2 = -\vartheta(A_1t_1 + A_2t_2 + A_3t_3 + H_1c_1 + H_2c_2 + H_3c_3,$$

$$L_3 = B_1t_1(\theta^2 + \vartheta^2) + B_2t_2(\theta^2 + \vartheta^2) + B_3t_3(\theta^2 + \vartheta^2) + I_1c_1(\theta^2 + \vartheta^2) + I_2c_2(\theta^2 + \vartheta^2) + I_3c_3(\theta^2 + \vartheta^2) + q_0, \quad (24)$$

$$L_4 = D_1t_1(\theta^2 + \vartheta^2) + D_2t_2(\theta^2 + \vartheta^2) + D_3t_3(\theta^2 + \vartheta^2) + J_1c_1(\theta^2 + \vartheta^2) + J_2c_2(\theta^2 + \vartheta^2) + Jc_3(\theta^2 + \vartheta^2) + q_0,$$

$$L_5 = O_1c_1 + O_2c_2 + O_3c_3 + X_1t_1 + X_2t_2 + X_3t_3,$$

where

$$\{A_1, A_2, B_2\} = \sum_{n=1}^{3}\int_{h_{n-1}}^{h_n} \frac{E^{(n)}(1+2v)}{1-v^2}\alpha^{(n)}\left\{1, \frac{z}{h}, \frac{z^2}{h}\right\}\mathrm{d}z,$$
$$B_1 = hA_2,$$

$$\{A_3, B_3\} = \sum_{n=1}^{3}\int_{h_{n-1}}^{h_n} \frac{E^{(n)}(1+2v)}{1-v^2}\alpha^{(n)}\varphi(z)\left\{\frac{1}{h}, \frac{z}{h}\right\}\mathrm{d}z, \quad (25)$$

$$\begin{Bmatrix} D_1, D_2, D_3 \\ X_1, X_2, X_3 \end{Bmatrix} = \sum_{n=1}^{3}\int_{h_{n-1}}^{h_n} \frac{E^{(n)}(1+2v)}{1-v^2}\alpha^{(n)}\left\{1, \frac{z}{h}, \frac{\varphi(z)}{h}\right\}\begin{Bmatrix} \Phi(z) \\ g'(z) \end{Bmatrix}\mathrm{d}z,$$

$$\{H_1, H_2, I_2\} = \sum_{n=1}^{3}\int_{h_{n-1}}^{h_n} \frac{E^{(n)}(1+2v)}{1-v^2}\eta^{(n)}\left\{1, \frac{z}{h}, \frac{z^2}{h}\right\}\mathrm{d}z,$$
$$I_1 = hH_2,$$

$$\{H_3, I_3\} = \sum_{n=1}^{3}\int_{h_{n-1}}^{h_n} \frac{E^{(n)}(1+2v)}{1-v^2}\eta^{(n)}\varphi(z)\left\{\frac{1}{h}, \frac{z}{h}\right\}\mathrm{d}z, \quad (26)$$

$$\begin{Bmatrix} J_1, J_2, J_3 \\ O_1, O_2, O_3 \end{Bmatrix} = \sum_{n=1}^{3}\int_{h_{n-1}}^{h_n} \frac{E^{(n)}(1+2v)}{1-v^2}\eta^{(n)}\left\{1, \frac{z}{h}, \frac{\varphi(z)}{h}\right\}\begin{Bmatrix} \Phi(z) \\ g'(z) \end{Bmatrix}\mathrm{d}z.$$

Table 1 Comparison of non-dimensional deflection $\frac{h}{\alpha_0 t_2 a^2}u_3(\frac{a}{2}, \frac{b}{2})$ of titanium/zirconia FGM sandwich plate under thermal load ($t_2 = 100$ °C, $\nu = 0.3$, $\frac{a}{b} = 1$, $\frac{a}{h} = 10$, $k_e = k_s = t_3 = c_1 = c_2 = c_3 = 0$)

k	Source	Face-core-face			
		1-0-1	1-1-1	1-2-1	2-1-2
0	Zenkour and Alghamdi (2008)	0.480262	0.480262	0.480262	0.480262
	TPT	0.477885	0.477885	0.477885	0.477885
	SPT	0.482292	0.482292	0.482292	0.482292
	Present	0.576119	0.576119	0.576119	0.576119
1	Zenkour and Alghamdi (2008)	0.636891	0.606256	0.582302	0.621067
	TPT	0.634039	0.603656	0.579865	0.618348
	SPT	0.645297	0.616924	0.593640	0.630778
	Present	0.780718	0.749624	0.719987	0.765562
2	Zenkour and Alghamdi (2008)	0.671486	0.639325	0.609829	0.665115
	TPT	0.668372	0.636549	0.607301	0.653171
	SPT	0.678375	0.650411	0.622721	0.665261
	Present	0.820709	0.793941	0.758666	0.809802
3	Zenkour and Alghamdi (2008)	0.683560	0.653638	0.622420	0.670253
	TPT	0.680313	0.650751	0.619826	0.667176
	SPT	0.689084	0.664265	0.635690	0.678352
	Present	0.832159	0.812675	0.776493	0.826263
x	Zenkour and Alghamdi (2008)	0.688795	0.661260	0.629487	0.677303
	TPT	0.685476	0.658302	0.626846	0.674147
	SPT	0.693445	0.671371	0.642819	0.684557
	Present	0.835712	0.822310	0.786525	0.833574

By solving the system of algebraic Eqs. (22), one can easily obtain the functions $U_{mr}, V_{mr}, W_{mrb}, W_{mrs}$ and Z_{mr} in terms of the hygrothermal and foundation parameters. In addition, the stresses $\sigma_x, \sigma_y, \sigma_z, \tau_{xy}, \tau_{yz}$ and τ_{xz} can be expressed in terms of $U_{mr}, V_{mr}, W_{mrb}, W_{mrs}$ and Z_{mr} as

$$\sigma_x^{(n)} = \frac{E^{(n)}}{(1+v)(-1+2v)}\Big[-U_{mr}\theta - vU_{mr}\theta + vV_{mr}\vartheta + (W_{mrb}z + W_{mrs}\Phi)((v+1)\theta^2 + \vartheta^2 v) + (1+v)\alpha^{(n)}\left(t_1 + \frac{z}{h}t_2 + \frac{\varphi}{h}t_3\right) + (1+v)\eta^{(n)}\left(c_1 + \frac{z}{h}c_2 + \frac{\varphi}{h}c_3\right) + \Phi'' Z_{mr}\Big]\sin(\theta x)\sin(\vartheta y), \quad (27a)$$

$$\sigma_y^{(n)} = \frac{E^{(n)}}{(1+v)(-1+2v)}\Big[-V_{mr}\vartheta - vU_{mr}\theta + vV_{mr}\vartheta + (W_{mrb}z + W_{mrs}\Phi)((v+1)\theta^2 + \vartheta^2 v) - (1+v)\alpha^{(n)}\left(t_1 + \frac{z}{h}t_2 + \frac{\varphi}{h}t_3\right) - (1+v)\eta^{(n)}\left(c_1 + \frac{z}{h}c_2 + \frac{\varphi}{h}c_3\right) + \Phi'' Z_{mr}\Big]\sin(\theta x)\sin(\vartheta y), \quad (27b)$$

$$\sigma_z^{(n)} = \frac{E^{(n)}}{(1+v)(-1+2v)}\Big[-vU_{mr}\theta + vV_{mr}\vartheta + (W_{mrb}z + W_{mrs}\Phi)((v+1)\theta^2 + \vartheta^2 v) - (1+v)\alpha^{(n)}\left(t_1 + \frac{z}{h}t_2 + \frac{\varphi}{h}t_3\right) - (1+v)\eta^{(n)}\left(c_1 + \frac{z}{h}c_2 + \frac{\varphi}{h}c_3\right) + (1-v)\Phi'' Z_{mr}\Big]\sin(\theta x)\sin(\vartheta y), \quad (27c)$$

Table 2 Non-dimensional deflection $\bar{u}_3$ of (1-1-1) FGM sandwich plate under thermal and hygrothermal loads $(z = 0, k = 1,\ \frac{a}{b} = 1)$

a/h	k_s	k_e	Thermal ($c_1 = c_2 = c_3 = 0$)			Hygrothermal ($t_2 = 100$°C)		
			$t_3 = 100$	$t_3 = 200$	$t_3 = 300$	$c_3 = 0.01$	$c_3 = 0.02$	$c_3 = 0.03$
10	0	0	6.36750	8.39558	10.42365	14.86371	23.35991	31.85611
		100	4.51813	5.95424	7.39035	10.54644	16.57475	22.60306
		200	3.48717	4.59327	5.69938	8.13969	12.79222	17.44475
	10	0	3.50823	4.62107	5.73392	8.18886	12.86949	17.55012
		100	2.84388	3.74407	4.64427	6.63797	10.43205	14.22614
		200	2.38415	3.13719	3.89023	5.56476	8.74536	11.92597
	20	0	2.39434	3.15064	3.90694	5.58853	8.78273	11.97692
		100	2.05477	2.70238	3.34999	4.79583	7.53690	10.27796
		200	1.79541	2.36000	2.92459	4.19037	6.58533	8.98029
20	0	0	6.38156	8.41901	10.4564	14.89827	23.41497	31.93168
		100	4.58589	6.04932	7.51275	10.70606	16.82624	22.94641
		200	3.57540	4.71581	5.85621	8.34695	13.11850	17.89004
	10	0	3.59611	4.74314	5.89016	8.39530	13.19449	17.99368
		100	2.94142	3.87916	4.81690	6.86684	10.79227	14.71770
		200	2.48669	3.27908	4.07146	5.80525	9.12380	12.44235
	20	0	2.49678	3.29239	4.08800	5.82880	9.16081	12.49283
		100	2.16005	2.84802	3.53598	5.04266	7.92527	10.80788
		200	1.90235	2.50793	3.11352	4.44103	6.97970	9.51838
30	0	0	6.38415	8.42333	10.46251	14.90462	23.42510	31.94557
		100	4.59846	6.06695	7.53545	10.73568	16.87289	23.01011
		200	3.59184	4.73863	5.88541	8.38557	13.17930	17.97303
	10	0	3.61248	4.76587	5.91925	8.43376	13.25505	18.07633
		100	2.95964	3.90438	4.84913	6.90961	10.85958	14.80956
		200	2.50589	3.30563	4.10536	5.85028	9.19466	12.53904
	20	0	2.51596	3.31891	4.12186	5.87378	9.23160	12.58942
		100	2.17979	2.87531	3.57082	5.08895	7.99810	10.90725
		200	1.92243	2.53569	3.14895	4.48808	7.05374	9.61940

Table 3 Non-dimensional in-plane normal stress $\sigma_1$of (1-1-1) FGM sandwich plate under thermal and hygrothermal loads $(z = \frac{h}{2},\ k = 1,\ \frac{a}{b} = 1,\ \frac{a}{h} = 10)$

a/h	k_s	k_e	Thermal ($c_1 = c_2 = c_3 = 0$)			Hygrothermal ($t_2 = 100$°C)		
			$t_3 = 100$	$t_3 = 200$	$t_3 = 300$	$c_3 = 0.01$	$c_3 = 0.02$	$c_3 = 0.03$
10	0	0	2.32667	2.68792	3.04916	4.23915	6.15162	8.06410
		100	3.55404	4.30815	5.06226	7.10437	10.65471	14.20504
		200	4.23826	5.21138	6.18450	8.70165	13.16505	17.62844
	10	0	4.22428	5.19293	6.16158	8.66903	13.11377	17.55852
		100	4.66519	5.77497	6.88475	9.69830	14.73141	19.76453
		200	4.97029	6.17773	7.38517	10.41055	15.85081	21.29108
	20	0	4.96353	6.16881	7.37409	10.39477	15.82602	21.25726
		100	5.18889	6.46630	7.74372	10.92086	16.65283	22.38481
		200	5.36102	6.69353	8.02604	11.32269	17.28436	23.24602
20	0	0	0.58355	0.67460	0.76565	1.06415	1.54476	2.02536
		100	0.88891	1.07758	1.26624	1.77706	2.66520	3.55335
		200	1.06075	1.30435	1.54794	2.17823	3.29572	4.41320
	10	0	1.05723	1.29970	1.54217	2.17001	3.28280	4.39558
		100	1.16856	1.44662	1.72468	2.42993	3.69130	4.95268
		200	1.24589	1.54867	1.85145	2.61046	3.97504	5.33961
	20	0	1.24417	1.54640	1.84864	2.60646	3.96874	5.33103
		100	1.30143	1.62197	1.94251	2.74014	4.17885	5.61756
		200	1.34526	1.67980	2.01435	2.84245	4.33965	5.83685
30	0	0	0.25951	0.30003	0.34056	0.68712	0.68712	0.90093
		100	0.39510	0.47896	0.56283	1.18466	1.18466	1.57943
		200	0.47154	0.57983	0.68812	1.46513	1.46513	1.96192
	10	0	0.46997	0.57776	0.68555	1.45937	1.45937	1.95408
		100	0.51954	0.64318	0.76681	1.64127	1.64127	2.20214
		200	0.55400	0.68864	0.82329	1.76770	1.76770	2.37455
	20	0	0.55323	0.68763	0.82203	1.76489	1.76489	2.37072
		100	0.57876	0.72132	0.86388	1.85856	1.85856	2.49845
		200	0.59830	0.74711	0.89591	1.93026	1.93026	2.59625

$$\sigma_{xy} = \frac{E^{(n)}}{2(1+v)}\left[\Phi' Z_{mr} + W_{mrs} - \frac{\Phi'}{h} W_{mrs}\right] sin(\theta x)\, si\, n(\vartheta y), \tag{27d}$$

$$\sigma_{yz} = \frac{E^{(n)}}{2(1+v)}\left[\Phi' Z_{mr} + W_{mrs} - \frac{\Phi'}{h} W_{mrs}\right] cos(\theta x)\, si\, n(\vartheta y), \tag{27e}$$

$$\sigma_{xz} = \frac{E^{(n)}}{2(1+v)}\left[2W_{mrb} z\theta\vartheta + 2\Phi W_{mrs}\theta\vartheta - U_{mr}\vartheta - V_{mr}\theta\right] cos(\theta x)\, cos(\vartheta y). \tag{27f}$$

Table 4 Non-dimensional transverse normal stress σ_3 of (1-1-1) FGM sandwich plate under thermal and hygrothermal loads $(z = \frac{h}{2},\ k = 1,\ \frac{a}{b} = 1,\ \frac{a}{h} = 10)$

a/h	k_s	k_e	Thermal ($c_1 = c_2 = c_3 = 0$)			Hygrothermal ($t_2 = 100$°C)		
			$t_3 = 100$	$t_3 = 200$	$t_3 = 300$	$c_3 = 0.01$	$c_3 = 0.02$	$c_3 = 0.03$
10	0	0	3.48645	4.16816	4.84987	6.94225	10.39805	13.85385
		100	4.19345	5.10146	6.00948	8.59270	12.99196	17.39122
		200	4.58758	5.62175	6.65592	9.51278	14.43799	19.36320
	10	0	4.57952	5.61112	6.64272	9.49399	14.40845	19.32292
		100	4.83350	5.94639	7.05928	10.08688	15.34026	20.59364
		200	5.00925	6.17840	7.34754	10.49716	15.98507	21.47298
	20	0	5.00536	6.17326	7.34116	10.48807	15.97079	21.45350
		100	5.13517	6.34462	7.55407	10.79111	16.44706	22.10300
		200	5.23432	6.47551	7.71670	11.02257	16.81083	22.59909
20	0	0	0.87315	1.04413	1.21511	1.73911	2.60507	3.47104
		100	1.04797	1.27484	1.50170	2.14725	3.24653	4.34581
		200	1.14635	1.40467	1.66298	2.37693	3.60751	4.83809
	10	0	1.14433	1.40200	1.65968	2.37222	3.60011	4.82800
		100	1.20807	1.48612	1.76417	2.52103	3.83398	5.14694
		200	1.25234	1.54454	1.83674	2.62438	3.99642	5.36846
	20	0	1.25136	1.54325	1.83513	2.62209	3.99282	5.36354
		100	1.28414	1.58651	1.88887	2.69862	4.11310	5.52759
		200	1.30923	1.61962	1.93000	2.75720	4.20516	5.65313
30	0	0	0.38819	0.46423	0.54027	0.77323	1.15827	1.54330
		100	0.46573	0.56655	0.66737	0.95426	1.44278	1.93131
		200	0.50944	0.62423	0.73902	1.05630	1.60317	2.15003
	10	0	0.50855	0.62305	0.73755	1.05421	1.59988	2.14555
		100	0.53689	0.66045	0.78402	1.12040	1.70390	2.28740
		200	0.55660	0.68645	0.81631	1.16640	1.77619	2.38599
	20	0	0.55616	0.68588	0.81560	1.16537	1.77459	2.38380
		100	0.57076	0.70514	0.83952	1.19945	1.82815	2.45685
		200	0.58193	0.719892	0.85784	1.22555	1.86916	2.51277

Table 5 Non-dimensional transverse shear stress σ_5 of (1-1-1) FGM sandwich plate under thermal and hygrothermal loads $(z = 0,\ k = 1,\ \frac{a}{b} = 1,\ \frac{a}{h} = 10)$

a/h	k_s	k_e	Thermal ($c_2 = 0$)			Hygrothermal ($t_2 = 100$°C)		
			$t_2 = 100$	$t_2 = 200$	$t_2 = 300$	$c_2 = 0.01$	$c_2 = 0.02$	$c_2 = 0.03$
10	0	0	-0.28339	-0.30166	-0.31993	-0.61105	-0.93871	1.26637
		100	1.30615	1.79668	2.28720	3.09966	4.89318	6.68670
		200	2.19227	2.96644	3.74061	5.16828	8.14429	11.12030
	10	0	2.17417	2.94255	3.71092	5.12603	8.07788	11.02974
		100	2.74518	3.69633	4.64749	6.45903	10.17288	13.88672
		200	3.14032	4.21795	5.29558	7.38146	11.62260	15.86374
	20	0	3.13157	4.20640	5.28123	7.36103	11.59049	15.81994
		100	3.42343	4.59168	5.75993	8.04236	12.66129	17.28022
		200	3.64635	4.88595	6.12556	8.56276	13.47916	18.39557
20	0	0	-0.07124	-0.07597	-0.08070	-0.15368	-0.23612	-0.31856
		100	0.32571	0.44787	0.57004	0.77305	1.22039	1.66773
		200	0.54909	0.74266	0.93623	1.29456	2.04003	2.78550
	10	0	0.54451	0.73662	0.92873	1.28387	2.02323	2.76259
		100	0.68924	0.92761	1.16599	1.62175	2.55427	3.48678
		200	0.78976	1.06027	1.33077	1.85643	2.92310	3.98978
	20	0	0.78753	1.05732	1.32712	1.85122	2.91492	3.97862
		100	0.86197	1.15556	1.44915	2.02501	3.18805	4.35110
		200	0.91893	1.23074	1.54254	2.15801	3.39708	4.63616
30	0	0	-0.03169	-0.03381	-0.03592	-0.06837	-0.10506	-0.14174
		100	0.14469	0.19894	0.25320	0.34342	0.54215	0.74088
		200	0.24412	0.33015	0.41618	0.57555	0.90699	1.23843
	10	0	0.24208	0.32746	0.41284	0.57079	0.89951	1.22823
		100	0.30656	0.41256	0.51855	0.72135	1.13613	1.55091
		200	0.35138	0.47170	0.59202	0.82599	1.30059	1.77519
	20	0	0.35039	0.47039	0.59038	0.82366	1.29694	1.77021
		100	0.38360	0.51421	0.64482	0.90119	1.41878	1.93637
		200	0.40902	0.54775	0.68649	0.96054	1.51206	2.06358

5. Numerical results

In this section, the effects of the temperature, humidity and elastic foundation parameters on the deflection and stresses of simply supported FGM sandwich plates resting on Pasternak foundations are discussed. The analysis is carried out for the following data (unless otherwise stated) $\frac{b}{a} = 1,\ \frac{a}{h} = 10, k_e = 50, k_s = 5,\ q_0 = 1, t_1 = 0, t_2 = t_3 = 100$ °C, $c_1 = 0, c_2 = c_3 = 0.01$ %, $T_0 = H_0 = 0,\ k = 1, h = 0.005$ m. Note that, the deflection u_3 is calculated at $x = a/2$ and $y = b/2$, while the in-plane normal stress σ_x at $x = a/2$, $y = b/2$ and $z = h/2$, also, the

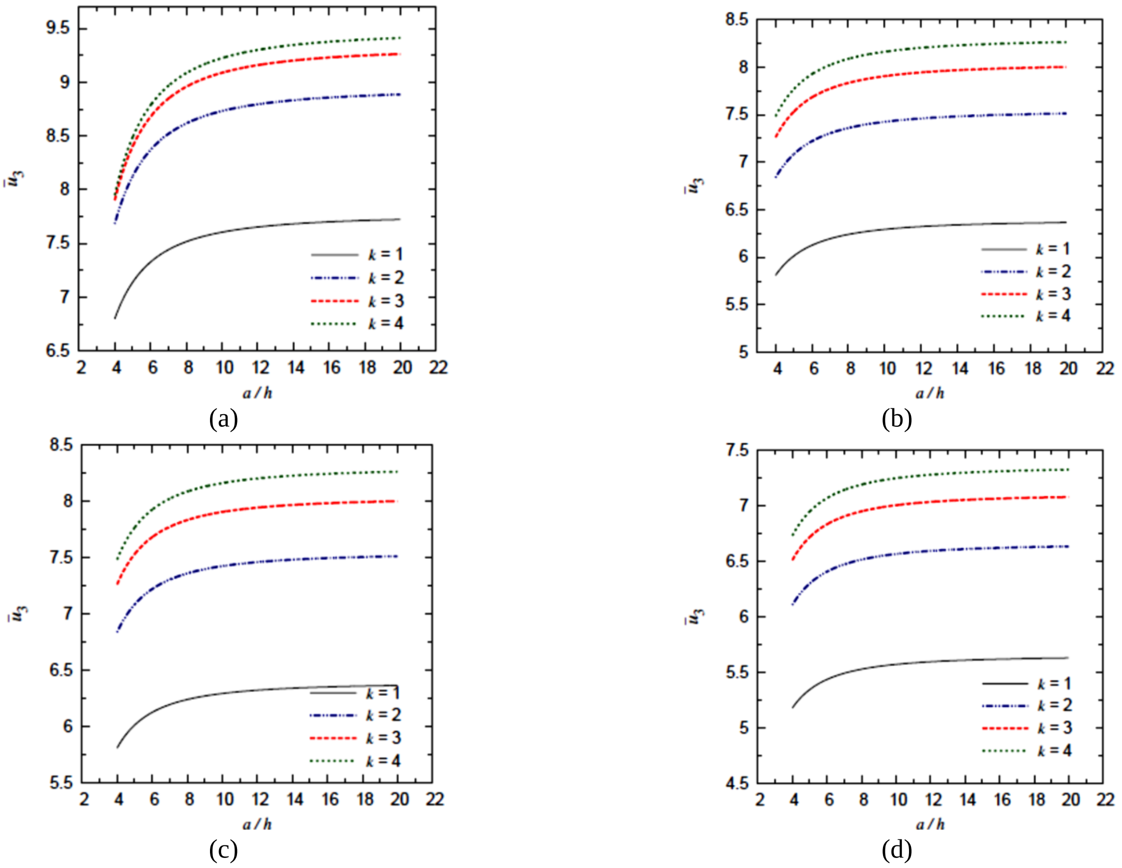

Fig. 2 Non-dimensional deflection $\bar{u}_3$ of (a) 2-1-2, (b) 1-1-1, (c) 1-2-1 and (d) 1-3-1 FGM sandwich plates versus the side-to-thickness ratio $\frac{a}{h}$ for various values of the power law index k

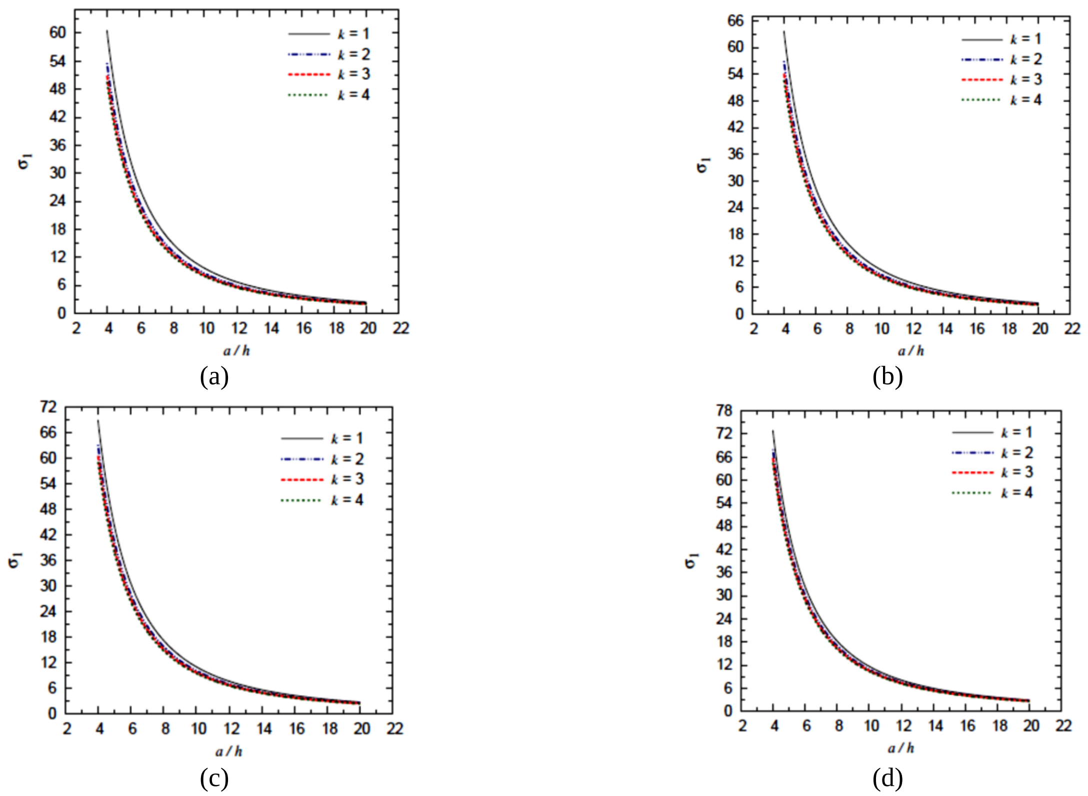

Fig. 3 Non-dimensional in-plane normal stress σ_1 of (a) 2-1-2, (b) 1-1-1, (c) 1-2-1 and (d) 1-3-1 FGM sandwich plates versus the side-to-thickness ratio $\frac{a}{h}$ for various values of the power law index k

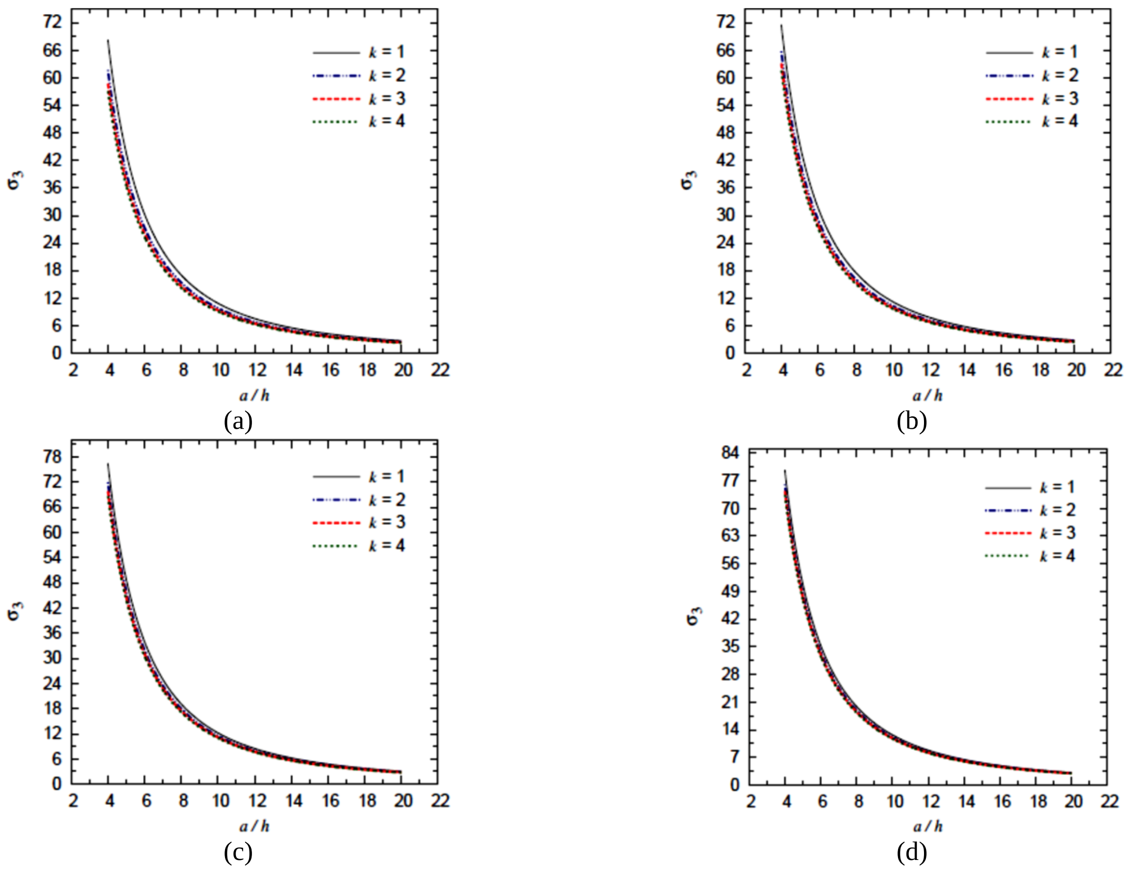

Fig. 4 Non-dimensional transverse normal stress σ_3 of (a) 2-1-2, (b) 1-1-1, (c) 1-2-1 and (d) 1-3-1 FGM sandwich plates versus the side-to-thickness ratio $\frac{a}{h}$ for various values of the power law index k

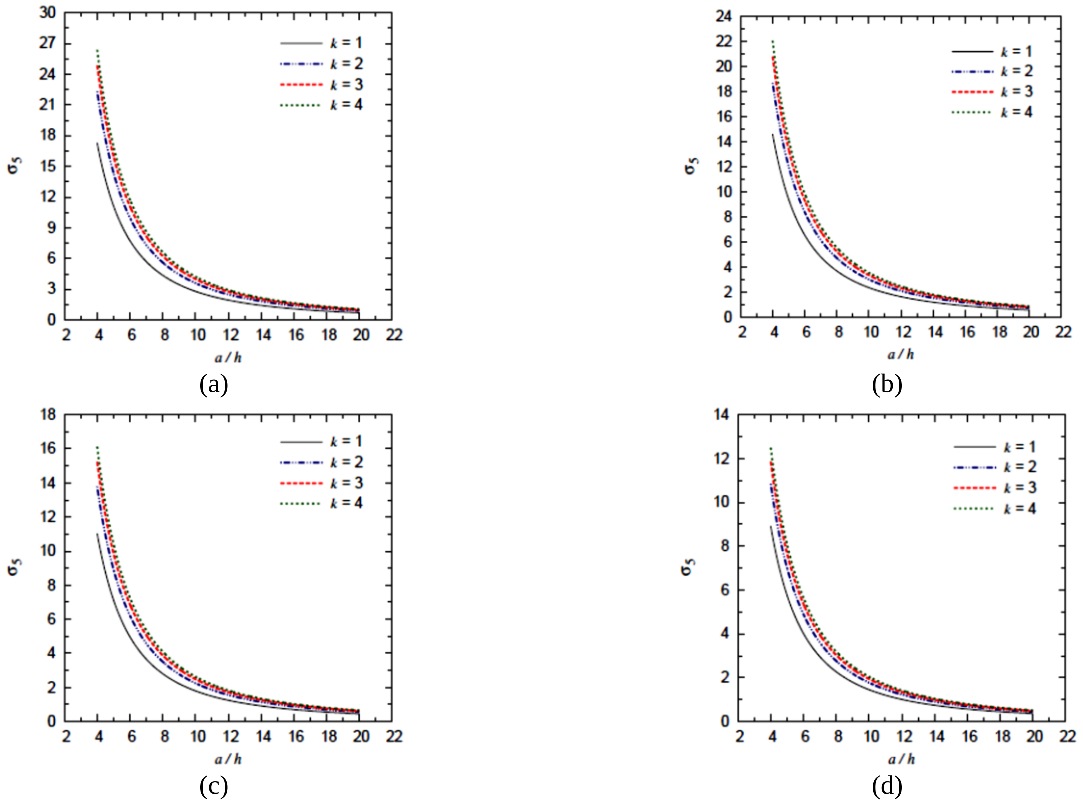

Fig. 5 Non-dimensional transverse shear stress σ_5 of (a) 2-1-2, (b) 1-1-1, (c) 1-2-1 and (d) 1-3-1 FGM sandwich plates versus the side-to-thickness ratio $\frac{a}{h}$ for various values of the power law index k

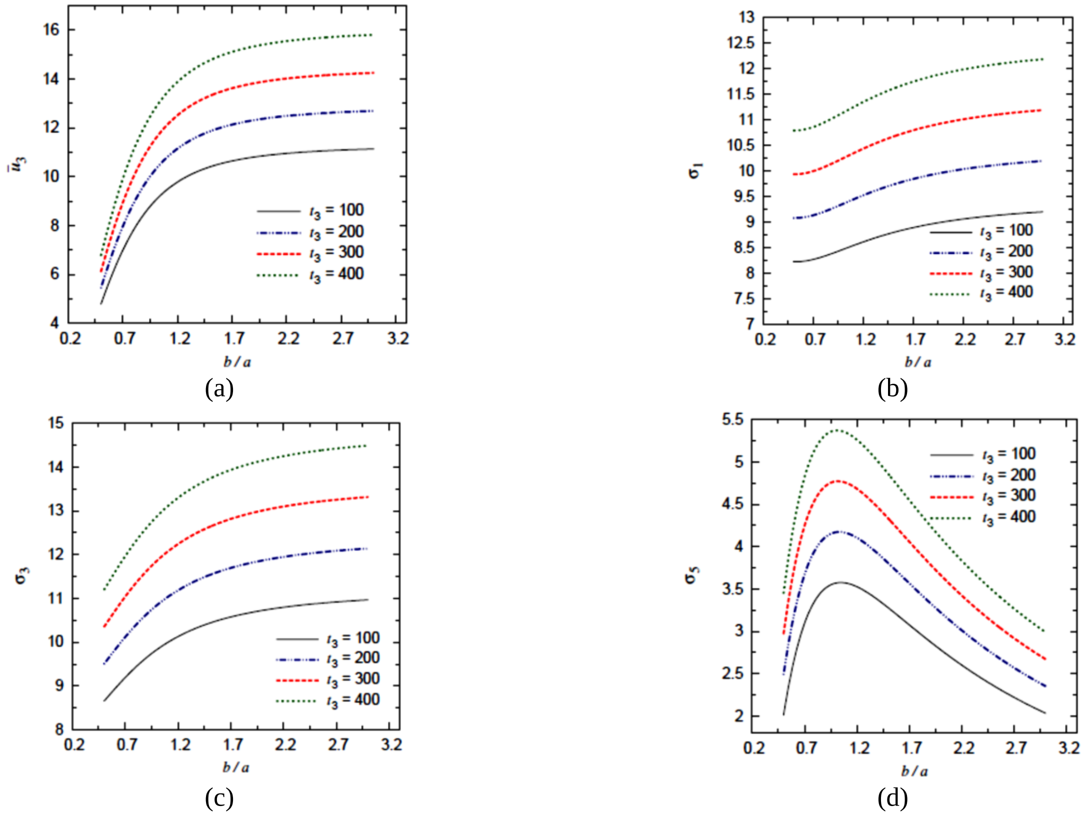

Fig. 6 Non-dimensional (a) deflection $\bar{u}_3$, (b) in-plane normal stress σ_1, (c) transverse normal stress σ_3 and (d) transverse shear stress σ_5 of (1-1-1) FGM sandwich plates versus the aspect ratio $\frac{b}{a}$ for various values of the temperature t_3

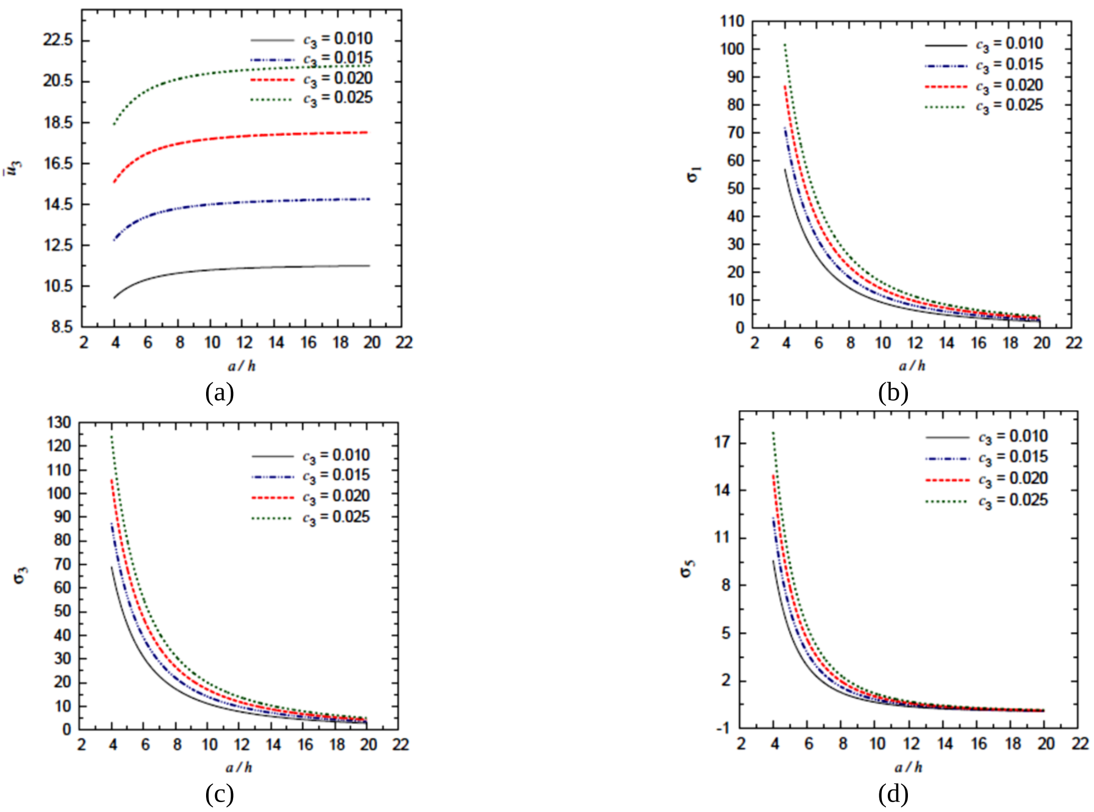

Fig. 7 Non-dimensional (a) deflection $\bar{u}_3$, (b) in-plane normal stress σ_1, (c) transverse normal stress σ_3 and (d) transverse shear stress σ_5 of (1-1-1) FGM sandwich plates versus the side-to-thickness ratio $\frac{a}{h}$ for various values of the moisture concentration c_3

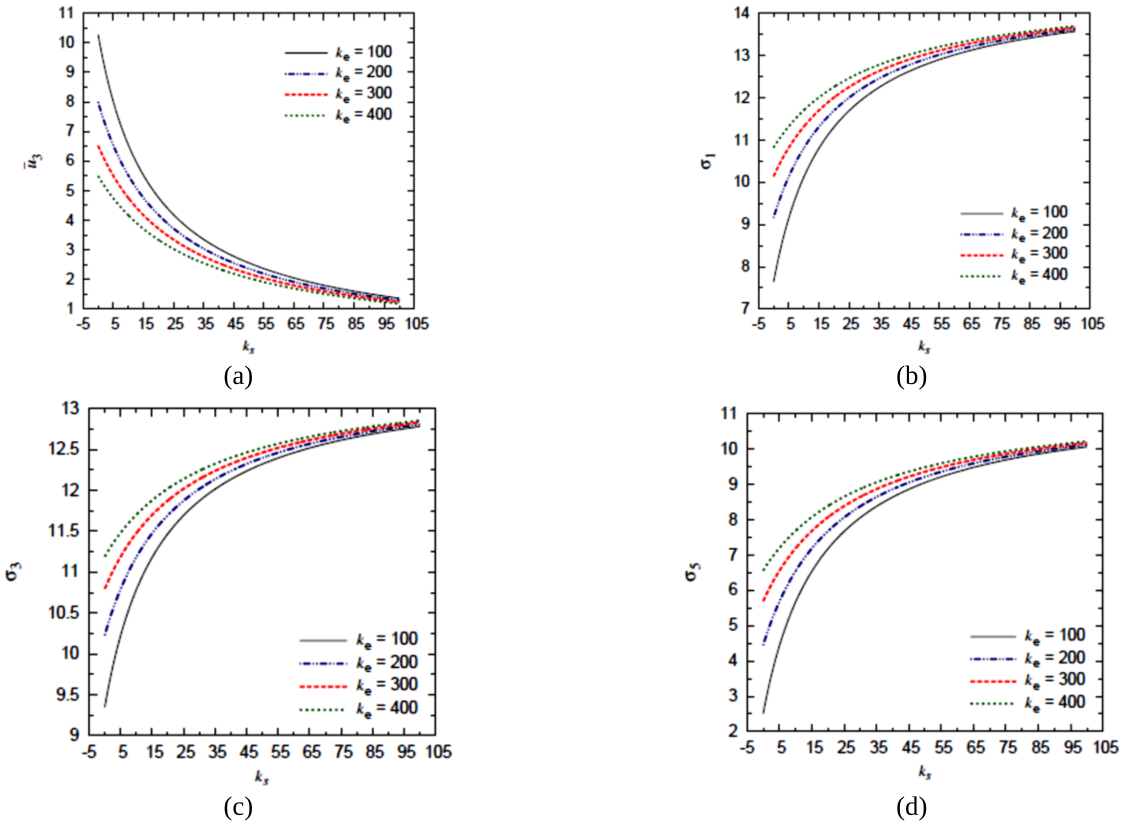

Fig. 8 Non-dimensional (a) deflection $\bar{u}_3$, (b) in-plane normal stress σ_1, (c) transverse normal stress σ_3 and (d) transverse shear stress σ_5 of (1-1-1) FGM sandwich plates subjected to hygrothermal loads versus the shear layer stiffness k_s for various values of the springs stiffness k_e

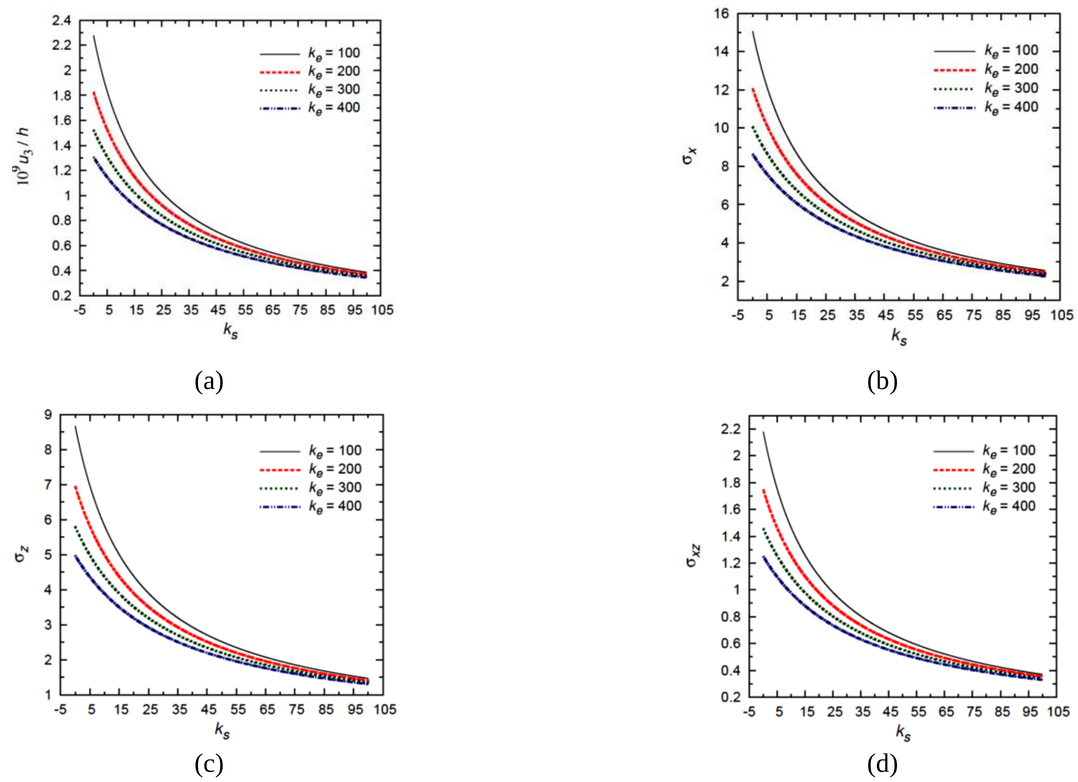

Fig. 9(a) deflection u_3, (b) in-plane normal stress σ_x, (c) transverse normal stress σ_z and (d) transverse shear stress σ_{xz} of (1-1-1) FGM sandwich plates without hygrothermal conditions versus the shear layer stiffness k_s for various values of the springs stiffness k_e

transverse shear stress σ_{xz} at $x = 0$, $y = b/2$ and $z = 0$.

The present FGM sandwich plates are composed of Titanium (metal) and Zirconia (ceramic) materials. The material properties of Titanium are: $E_m = 66.2\,E_0$, , $\alpha_m = 10.3\,\alpha_0$, $\eta_m = 0.44\,(\text{wt.}\%\,\text{H}_2\text{O})^{-1}$ and $\nu = 0.3$. While, the properties of Zirconia are: $E_c = 117.0\,E_0$, $\alpha_c = 7.11\,\alpha_0$, $\eta_c = 0.001\,(\text{wt.}\%\,\text{H}_2\text{O})^{-1}$ and $\nu = 0.3$; in which $E_0 = 10^9$ Pa and $\alpha_0 = 10^{-6}$ (1/°C).

The following non-dimensional parameters are used in the present study

$$\bar{u}_3 = \frac{hu_3}{a^2\alpha_0 t_2}, \sigma_1 = -\frac{h^2\sigma_x}{10a^2E_0\alpha_0 t_2},$$

$$\sigma_3 = -\frac{h^2\sigma_z}{10a^2E_0\alpha_0 t_2}, \sigma_5 = -\frac{h\sigma_{xz}}{10aE_0\alpha_0 t_2}, \tag{28}$$

$$k_e = \frac{K_e a^4}{D_c}, \quad k_s = \frac{K_s a^2}{D_c}, \quad D_c = \frac{E_c h^3}{12(1-\nu^2)}$$

Table 1 contains a comparison example for titanium/zirconia FGM sandwich plates under linear distributed thermal loading ($t_2 = 100\,^{\circ}$C). For different values of the power law index k and various types of the sandwich plates, the non-dimensional deflection $\frac{hu_3}{\alpha_0 t_2 a^2}$ presented by the present refined plate theory (RPT) is compared with that predicted by Zenkour and Alghamdi (2008) using the SPT. The results of proposed theory agree well with those of Zenkour and Alghamdi (2008). Next, parametric studies are introduced in tabular form (see, Tables 2-5) and graphical form (see, Figs. 2-9) to investigate the effects of various parameters, such as the power law index, elastic foundation stiffness, temperature, humidity, core thickness, side-to-thickness ratio and plate aspect ratio, on the deflection and stresses of titanium/zirconia FGM sandwich plates. Tables 2-5 show the variation of the deflection $\bar{u}_3$, longitudinal stress σ_1 transverse normal stress σ_3, and transverse shear stress σ_5 of (1-1-1) sandwich plate under thermal and hygrothermal loads for different values of the elastic springs stiffness k_e and shear layer stiffness k_s. It can be seen that the results of the FGM sandwich plate under hygrothermal load are greater than those of the plate under thermal load. Moreover, the elevated temperature and moisture concentration lead to weaken the structure of the plate, subsequently, the deflection and stresses increase with increasing the temperature or/and moisture. Further, with increasing the Pasternak foundation coefficients (k_e and k_s) the central deflection $\bar{u}_3$ decreases while the stresses σ_1, σ_3 and σ_5 increase. Figs. 2-5 display, respectively, the effect of the power law index k on the central deflection $\bar{u}_3$, longitudinal stress σ_1, transverse normal stress σ_3 and transverse shear stress σ_5 of various types of FGM sandwich plates. The deflection is plotted versus the side-to-thickness ratio varying from 4 to 20. It is clear that, for all types of sandwich plates, the deflection is increasing as the ratio $\frac{a}{h}$ is increasing. While, the stresses decrease as the ratio $\frac{a}{h}$ increases. Obviously, Figs. 2-5 reveal the sensitivity of the deflection and stresses to the variation of the parameter k. The central deflection and the transverse shear stress σ_5 increase whereas the normal stresses σ_1 and σ_3 decrease as the power law index k increases.

The variations of central deflection $\bar{u}_3$, longitudinal stress σ_1, transverse normal stress σ_3 and transverse shear stress σ_5 of (1-1-1) FGM sandwich plate against the plate aspect ratio $\frac{b}{a}$ for different values of the temperature parameter t_3 are investigated in Figs. 6a,b,c and d, respectively. It can be noted that the deflection and the normal stresses monotonically increase with the increase of the ratio $\frac{b}{a}$ and the temperature parameter t_3. Whereas, the shear stress σ_5 increases to reach its maximum and then decreases as the ratio $\frac{b}{a}$ increases.

In Fig. 7, the influences of the moisture concentration c_3 and side-to-thickness ratio $\frac{a}{h}$ on the deflection $\bar{u}_3$ and stresses σ_1, σ_3 and σ_5 are illustrated. Similar to the effect of the temperature on the results, the deflection and the stresses σ_1, σ_3 and σ_5 are increasing as the moisture increases.

The effects of the Pasternak foundation parameters (k_e and k_s) individually on the deflection and stresses of the (1-1-1) FGM sandwich plate subjected to hygrothermal loads and without hygrothermal conditions are presented in Figs. 8 and 9, respectively. As it is shown in Fig. 8 and according to Tables 2-5, with considering the hygrothermal environment, the increase in the stiffness of the foundations leads to a decrement in the deflection and increments in the stresses. However, with ignoring the hygrothermal environment, the behavior of the stresses is reversed, i.e., the stresses have the same sense of the deflection with the variation of the elastic foundation parameters as shown in Fig. 9. Further, it is noticed that the effects of the variation of springs stiffness on the results are more significant for small values of the shear layer parameter.

5. Conclusions

The static bending of various types of FGM sandwich plates resting on two-parameter elastic foundations in hygrothermal environment is investigated. The present theory takes into account both shear and normal strains effects. Thus, it predicts results more accurate than the shear deformation plate theories. The results obtained by the shear and normal deformation theory are compared with those available in the literature and also with those obtained by other shear deformation theories. According to the comparison example, the present results are agreed well with the published ones. Numerical results show that the deflection and stresses are very sensitive to the variation of the power law index and the core thickness. With the increase of the power law index, the deflection and transverse shear stress are monotonically increasing, while the normal stresses decrease. The same behavior can be observed with the variation of the core thickness. An increment occurs in the deflection and normal stresses as the aspect ration increases. The deflection and stresses increase as the temperature and moisture increase. A decrement occurs in the deflection with the increase of the foundation stiffness whereas the stresses have a contrast response when the hygrothermal conditions are taken into account and have the same response when the hygrothermal environment is ignored. Moreover, for the small values of the shear layer stiffness, the effect of the springs stiffness is more pronounced.

References

Abazid, M.A. and Sobhy, M. (2018), "Thermo-electro-mechanical bending of FG piezoelectric microplates on Pasternak foundation based on a four-variable plate model and the modified couple stress theory", *Microsyst. Technol.*, **24**(2), 1227-1245.

Alibeigloo, A. and Liew, K.M. (2014), "Free vibration analysis of sandwich cylindrical panel with functionally graded core using three-dimensional theory of elasticity", *Compos. Struct.*, **113**, 23-30.

Anderson, T.A. (2003), "A 3-D elasticity solution for a sandwich composite with functionally graded core subjected to transverse loading by a rigid sphere", *Compos. Struct.*, **60**(3), 265-274.

Aragh, B.S. and Yas, M.H. (2011), "Effect of continuously grading fiber orientation face sheets on vibration of sandwich panels with FGM core", *Int. J. Mech. Sci.*, **53**(8), 628-638.

Arefi, M. and Zenkour, A.M. (2016), "Employing sinusoidal shear deformation plate theory for transient analysis of three layers sandwich nanoplate integrated with piezo-magnetic face-sheets", *Smart Mater. Struct.*, **25**(11), 115040.

Arefi, M. and Zenkour, A.M. (2017a), "Influence of micro-length-scale parameters and inhomogeneities on the bending, free vibration and wave propagation analyses of a FG Timoshenko's sandwich piezoelectric microbeam", *J. Sandw. Struct. Mater.*, 1099636217714181.

Arefi, M. and Zenkour, A.M. (2017b), "Size-dependent vibration and bending analyses of the piezomagnetic three-layer nanobeams", *Appl. Phys. A*, **123**(3), 202.

Arefi, M. and Zenkour, A.M. (2017c), "Thermo-electro-mechanical bending behavior of sandwich nanoplate integrated with piezoelectric face-sheets based on trigonometric plate theory", *Compos. Struct.*, **162**, 108-122.

Arefi, M. and Zenkour, A.M. (2017d), "Vibration and bending analysis of a sandwich microbeam with two integrated piezo-magnetic face-sheets", *Compos. Struct.*, **159**, 479-490.

Arefi, M. and Zenkour, A.M. (2017e), "Nonlocal electro-thermo-mechanical analysis of a sandwich nanoplate containing a Kelvin-Voigt viscoelastic nanoplate and two piezoelectric layers", *Acta Mech.*, **228**(2), 475-493.

Arefi, M. and Zenkour, A.M. (2017f), "Effect of thermo-magneto-electro-mechanical fields on the bending behaviors of a three-layered nanoplate based on sinusoidal shear-deformation plate theory", *J. Sandw. Struct. Mater.*, 1099636217697497.

Arefi, M. and Zenkour, A.M. (2017g), "Size-dependent electro-elastic analysis of a sandwich microbeam based on higher-order sinusoidal shear deformation theory and strain gradient theory", *J. Intell. Mater. Syst. Struct.*, 1045389X17733333.

Arefi, M. and Zenkour, A.M. (2017h), "Size-dependent free vibration and dynamic analyses of piezo-electro-magnetic sandwich nanoplates resting on viscoelastic foundation", *Phys. B*, **521**, 188-197.

Arefi, M. and Zenkour, A.M. (2017i), "Vibration and bending analyses of magneto-electro-thermo-elastic sandwich microplates resting on viscoelastic foundation", *Appl. Phys. A*, **123**(8), 550.

Arefi, M. and Zenkour, A.M. (2017j), "Thermo-electro-magneto-mechanical bending behavior of size-dependent sandwich piezomagnetic nanoplates", *Mech. Res. Comm.*, **84**, 27-42.

Arefi, M., and Zenkour, A.M. (2018), "Free vibration analysis of a three-layered microbeam based on strain gradient theory and three-unknown shear and normal deformation theory", *Steel Compos. Struct.*, **26**(4), 421-437.

Arefi, M., Bidgoli, E.M.R. and Zenkour, A.M. (2018), "Free vibration analysis of a sandwich nano-plate including FG core and piezoelectric face-sheets by considering neutral surface", *Mech. Adv. Mater. Struct.*, 1-12.

Aydogdu, M. (2009), "A new shear deformation theory for laminated composite plates", *Compos. Struct.*, **89**(1), 94-101.

Bouafia, K., Kaci, A., Houari, M.S.A., Benzair, A. and Tounsi, A. (2017), "A nonlocal quasi-3D theory for bending and free flexural vibration behaviors of functionally graded nanobeams", *Smart Struct. Syst.*, **19**(2), 115-126.

Bouderba, B., Houari, M.S.A., Tounsi, A. and Mahmoud, S.R. (2016), "Thermal stability of functionally graded sandwich plates using a simple shear deformation theory", *Struct. Eng. Mech.*, **58**(3), 397-422.

Carrera, E. (2002), "Theories and finite elements for multilayered, anisotropic, composite plates and shells", *Arch. Comput. Meth. Eng.*, **9**(2), 87-140.

Carrera, E. and Ciuffreda, A. (2005), "A unified formulation to assess theories of multilayered plates for various bending problems", *Compos. Struct.*, **69**(3), 271-293.

Chen, C.S., Liu, F.H. and Chen, W.R. (2017), "Vibration and stability of initially stressed sandwich plates with FGM face sheets in thermal environments", *Steel Compos. Struct.*, **23**(3), 251-261.

Cheng, Z.Q. and Batra, R.C. (2000), "Exact correspondence between eigenvalues of membranes and functionally graded simply supported polygonal plates", *J. Sound Vibr.*, **229**(4), 879-895.

Cunedioglu, Y. (2015), "Free vibration analysis of edge cracked symmetric functionally graded sandwich beams", *Struct. Eng. Mech.*, **56**(6), 1003-1020.

Das, M., Barut, A., Madenci, E. and Ambur, D.R. (2006), "A triangular plate element for thermo-elastic analysis of sandwich panels with a functionally graded core", *Int. J. Numer. Meth. Eng.*, **68**(9), 940-966.

Dozio, L. (2013), "Natural frequencies of sandwich plates with FGM core via variable-kinematic 2-D Ritz models", *Compos. Struct.*, **96**, 561-568.

Fard, K.M. (2014), "Higher order free vibration of sandwich curved beams with a functionally graded core", *Struct. Eng. Mech.*, **49**(5), 537-554.

Ferreira, A.J.M., Castro L.M.S. and Bertoluzza, S. (2003), "A high order collocation method for the static and vibration analysis of composite plates using a first-order theory", *Compos. Struct.*, **34**, 627-636.

Houari, M.S.A., Tounsi, A. and Anwer, B. (2013), "Thermoelastic bending analysis of functionally graded sandwich plates using a new higher order shear and normal deformation theory", *Int. J. Mech. Sci.*, **76**, 102-111.

Karama, M., Afaq, K.S. and Mistou, S. (2003), "Mechanical behavior of laminated composite beam by the new multi-layered laminated composite structures model with transverse shear stress continuity", *Int. J. Sol. Struct.*, **40**(6), 1525-1546.

Kashtalyan, M. and Menshykova, M. (2009), "Three-dimensional elasticity solution for sandwich panels with a functionally graded core", *Compos. Struct.*, **87**(1), 36-43.

Kirugulige, M.S., Kitey, R. and Tippur, H.V. (2005), "Dynamic fracture behavior of model sandwich structures with functionally graded core: A feasibility study", *Compos. Sci. Technol.*, **65**(7), 1052-1068.

Li, D., Deng, Z., Xiao, H. and Zhu, L. (2018), "Thermomechanical bending analysis of functionally graded sandwich plates with both functionally graded face sheets and functionally graded cores", *Mech. Adv. Mater. Struct.*, **25**(3), 179-191.

Li, Q., Lu, V. and Kou, K. (2008), "Three-dimensional vibration analysis of functionally graded material sandwich plates", *J. Sound Vibr.*, **311**(1-2), 498-515.

Meksi, R., Benyoucef, S., Mahmoudi, A., Tounsi, A., Adda Bedia, E.A. and Mahmoud, S.R. (2017), "An analytical solution for bending, buckling and vibration responses of FGM sandwich plates", *J. Sandw. Struct. Mater.*, 1099636217698443.

Meziane, M.A.A., Abdelaziz, H.H. and Tounsi, A. (2014), "An efficient and simple refined theory for buckling and free vibration of exponentially graded sandwich plates under various boundary conditions", *J. Sandw. Struct. Mater.*, **16**(3), 293-318.

Natarajan, S. and Manickam, G. (2012), "Bending and vibration of functionally graded material sandwich plates using an accurate theory", *Fin. Elem. Anal. Des.*, **57**, 32-42.

Radwan, A.F. (2017), "Effects of non-linear hygrothermal conditions on the buckling of FG sandwich plates resting on elastic foundations using a hyperbolic shear deformation theory", *J. Sandw. Struct. Mater.*, 1099636217693557.

Reddy, J.N. (1984), "A simple higher-order theory for laminated composite plates", *J. Appl. Mech.*, **51**(4), 745-752.

Reissner, E. (1945), "The effect of transverse shear deformation on the bending of elastic plates", *J. Appl. Mech. Trans.*, **12**, 69-77.

Shimpi, R.P. (2002), "Refined plate theory and its variants", *AIAA J.*, **40**(1), 137-146.

Sobhy, M. (2013), "Buckling and free vibration of exponentially graded sandwich plates resting on elastic foundations under various boundary conditions", *Compos. Struct.*, **99**, 76-87.

Sobhy, M. (2016), "An accurate shear deformation theory for vibration and buckling of FGM sandwich plates in hygrothermal environment", *Int. J. Mech. Sci.*, **110**, 62-77.

Sobhy, M. (2017), "Hygro-thermo-mechanical vibration and buckling of exponentially graded nanoplates resting on elastic foundations via nonlocal elasticity theory", *Struct. Eng. Mech.*, **63**(3), 401-415.

Sobhy, M. and Radwan, A.F. (2017), "A new quasi 3D nonlocal plate theory for vibration and buckling of FGM nanoplates", *Int. J. Appl. Mech.*, **9**(1), 1750008.

Sofiyev, A.H. (2014), "The vibration and buckling of sandwich cylindrical shells covered by different coatings subjected to the hydrostatic pressure", *Compos. Struct.*, **117**, 124-134.

Soldatos, K.P. (1992), "A transverse shear deformation theory for homogeneous monoclinic plates", *Acta Mech.*, **94**(3-4), 195-220.

Thai, H.T. and Vo, T.P. (2013), "A new sinusoidal shear deformation theory for bending, buckling, and vibration of functionally graded plates", *Appl. Math. Model.*, **37**(5), 3269-81.

Tounsi, A., Houari, M.S.A. and Benyoucef, S. (2013), "A refined trigonometric shear deformation theory for thermoelastic bending of functionally graded sandwich plates", *Aerosp. Sci. Technol.*, **24**(1), 209-20.

Tounsi, A., Houari, M.S.A. and Bessaim, A. (2016), "A new 3-unknowns non-polynomial plate theory for buckling and vibration of functionally graded sandwich plate", *Struct. Eng. Mech.*, **60**(4), 547-565.

Touratier, M. (1991), "An efficient standard plate theory", *Int. J. Eng. Sci.*, **29**(8), 901-916.

Zenkour, A.M. (2004), "Thermal effects on the bending response of fiber-reinforced viscoelastic composite plates using a sinusoidal shear deformation theory", *Acta Mech.*, **171**(3-4), 171-187.

Zenkour, A.M. (2005), "A comprehensive analysis of functionally graded sandwich plates: Part 1, deflection and stresses, part 2-buckling and free vibration", *Int. J. Sol. Struct.*, **42**(18-19), 5243-5258.

Zenkour, A.M. (2007), "Elastic deformation of the rotating functionally graded annular disk with rigid casing", *J. Mater. Sci.*, **42**, 9717-9724.

Zenkour, A.M. (2009a), "The effect of transverse shear and normal deformations on the thermomechanical bending of functionally graded sandwich plates", *Int. J. Appl. Mech.*, **1**(4), 667-707.

Zenkour, A.M. (2009b), "The refined sinusoidal theory for FGM plates on elastic foundations", *Int. J. Mech. Sci.*, **51**(11-12), 869-880

Zenkour, A.M. and Alghamdi, N.A. (2008), "Thermoelastic bending analysis of functionally graded sandwich plates", *J. Mater. Sci.*, **43**(8), 2574-2589

Zenkour, A.M. and Arefi, M. (2017), "Nonlocal transient electrothermomechanical vibration and bending analysis of a functionally graded piezoelectric single-layered nanosheet rest on visco-Pasternak foundation", *J. Therm. Stress.*, **40**(2), 167-184.

Zenkour, A.M. and Sobhy, M. (2012), "Elastic foundation analysis of uniformly loaded functionally graded viscoelastic sandwich plates", *J. Mech.*, **28**(3), 439-452.

Zenkour, A.M., Allam, M.N.M. and Sobhy, M. (2010), "Bending analysis of FG viscoelastic sandwich beams with elastic cores resting on Pasternak's elastic foundations", *Acta Mech.*, **212**(3-4), 233-252.

CC